

The Pattern of Disulfide Linkages in the Extracellular Loop Regions of Connexin 32 Suggests a Model for the Docking Interface of Gap Junctions

Cynthia I. Foote, Lan Zhou, Xing Zhu, and Bruce J. Nicholson

Department of Biological Sciences, State University of New York at Buffalo, Buffalo, New York 14260-1300

Abstract. Connexins, like true cell adhesion molecules, have extracellular domains that provide strong and specific homophilic, and in some cases, heterophilic interactions between cells. Though the structure of the binding domains of adhesion proteins have been determined, the extracellular domains of connexins, consisting of two loops of ~34–37 amino acids each, are not easily studied in isolation from the rest of the molecule. As an alternative, we used a novel application of site-directed mutagenesis in which four of the six conserved cysteines in the extracellular loops of connexin

32 were moved individually and in all possible pairwise and some quadruple combinations. This mapping allowed us to deduce that all disulfides form between the two loops of a single connexin, with the first cysteine in one loop connected to the third of the other. Furthermore, the periodicity of movements that produced functional channels indicated that these loops are likely to form antiparallel β sheets. A possible model that could explain how these domains from apposed connexins interact to form a complete channel is discussed.

GAP junctions are integral membrane proteins that form channels to allow passage of ions and small molecules between cells in contact. They are ubiquitously found in all metazoa and have been proposed to play roles in the processes of development (Guthrie and Gilula, 1989; Paul et al., 1995), cancer (Loewenstein and Rose, 1992; Yamasaki and Naus, 1996), and transmission of electrical signals in heart (Severs, 1994) and neurons (Dermietzel and Spray, 1993; Fulton, 1995). In vertebrates, gap junction channels are composed of subunits called connexins that form a dodecameric structure when two hexameric hemichannels dock in the narrow intercellular space separating adjacent cells. Hemichannels appear to assemble initially in the *trans*-Golgi (Musil and Goodenough, 1993) before transportation to the cell membrane, where docking and the formation of junctional plaques occur. This may be a process of random diffusion and trapping once apposed hemichannels dock, or lateral affinity between connexins. Alternatively, it could result from a directed process, possibly involving electrophoresis of the

hemichannels through the membrane as suggested in oocytes for connexin 32 (Cx32)¹ (Levine et al., 1993).

Studies on Cx26 (Zhang and Nicholson, 1994), Cx32 (Milks et al., 1988), and Cx43 (Yancey et al., 1989) have revealed that connexins share a similar membrane conformation consisting of four transmembrane regions with the NH₂ and COOH termini located cytoplasmically. Despite a number of structural studies on isolated gap junctions (Caspar et al., 1977; Makowski et al., 1977; Unwin and Zampighi, 1980; Sosinsky, 1992; Hoh et al., 1993), the resolution has remained at a level that provides little information on the folding of the polypeptide chain within individual subunits. Circular dichroism (CD) analysis (Casco et al., 1990) implicated α helices as the predominant component of the transmembrane segments. This interpretation is consistent with X-ray studies (Tibbitts et al., 1990), and is largely confirmed in a recent 7-Å resolution projection map of frozen, hydrated gap junctions (Yeager and Nicholson, 1996; Unger et al., 1997). This same level of structural detail has not been obtained for the extracellular domains where docking occurs, since projection maps are dominated by the transmembrane structures. Although three-dimensional reconstructions may help to resolve this, direct surface imaging of these domains is only possible after

C.I. Foote's present address is Dept. of Anatomy and Cell Biology, Emory University, 1648 Pierce Dr., Atlanta, GA 30322-3030.

Address all correspondence to Bruce J. Nicholson, Dept. of Biological Sciences, State University of New York at Buffalo, Cooke Hall, Box 601300, Buffalo, NY 14260-1300. Tel.: (716) 645-3344. Fax: (716) 645-3776. E-mail: bjn@acsu.buffalo.edu

1. *Abbreviations used in this paper:* Cx32, connexin 32; E1, extracellular loop 1; E2, extracellular loop 2; TM, transmembrane domain; wt, wild-type.

highly disruptive treatments required for splitting gap junctions (Manjunath et al., 1984; Ghoshroy et al., 1995; Perkins et al., 1997). Atomic force microscopy offers a more controlled, but still disruptive approach (Hoh et al., 1993). Nonetheless, results from these two techniques both show the extracellular surface to have six discrete protrusions. This suggests that the extracellular loops of each connexin must form a stable conformation, even in the hemichannel, for the structures evident in atomic force microscopy images of individual hemichannels to be reinforced in the extensively averaged images of Perkins et al. (1997).

Recently, greater interest has focused on the extracellular domains of connexins due to the implication of these highly conserved regions in both the specificity of hemichannel docking (Elfgang et al., 1995; White et al., 1995) as well as the regulation of voltage gating of the channel (Verselis et al., 1994). In the case of Cx43, -46, and -56, the specificity of heterotypic interactions between hemichannels composed of different connexins appears to be largely dictated by the primary sequence of the second extracellular loop (White et al., 1994). Although specific residues within the primary sequence are likely to play a role in docking specificity, the critical spatial relationships of individual residues are determined by the overall tertiary structure of these extracellular loop regions. Therefore, a clear understanding of their structure will be essential, not only for defining the basis of selective homophilic and heterophilic interactions between connexins (analogous to cadherins), but also for establishing how this leads to the unique seal between hemichannels that electrically isolates the intercellular channel from the extracellular environment.

The most notable feature of the extracellular domains of connexins are the six cysteine residues, three in each loop, which are conserved in all family members studied to date with only one exception (Cx31; Hoh et al., 1991). Dahl et al. (1992) demonstrated the importance of these conserved cysteines through individual mutations of each cysteine to a serine, resulting in a loss of channel function in all cases. This result, along with the extracellular location of these cysteines, suggests they are likely to be involved in disulfide bond formation. This is partly confirmed by two independent studies (John and Revel, 1991; Rahman and Evans, 1991), examining the mobility of intact and proteolyzed connexins in reducing and nonreducing SDS-PAGE. This approach demonstrated that at least one disulfide bond connects the two loops of a connexin, whereas none occur between connexin subunits.

If all six cysteines are involved in disulfide bonds within a connexin, at least seven permutations of disulfides are possible (see Fig. 1). Defining which of these combinations form in situ would represent a significant advance in defining the structure of these docking domains. Here, we approach this problem through a series of single or paired movements of the first and third cysteines of each loop. The logic followed is that, by analogy with the data of Dahl et al. (1992), movements of one cysteine should be nonfunctional, but could be rescued by the appropriate compensatory movement of a second cysteine to which the first was paired. This strategy has produced a mapping of most of the disulfides in the extracellular loops, and suggests that much of these domains may fold as β sheets. A

possible model of connexin docking is discussed consistent with available structural data on gap junctions that infer an interdigitation of the extracellular domains (Perkins et al., 1997; Unger et al., 1997).

Materials and Methods

Construction of Cx32 Mutants

The 1.5-kb Cx32 cDNA (Paul, 1986) was ligated into the M13mp18 phage vector at the EcoRI site. Using the site-directed mutagenesis procedure of Kunkel (1987), the cysteines at positions 63, 74, 178, and 189 were mutated to serine residues. In conjunction with this, a cysteine is substituted at positions between one and four residues to the NH_2 -terminal side of the original cysteines 63 and 178 (defined as the “-” direction), or a similar distance to the COOH-terminal side of cysteines 74 and 189 (defined as the “+” direction). Serine was chosen as the substitution likely to cause the least perturbation of structure, based on both preservation of side chain volume and general polarity. The oligonucleotides used to create the mutants, and the corresponding mutant designations used throughout, are: Extracellular loop 1 (E1):C₁-1 (C63S/I62C): 5'GGGTGTTAGAGCGAGAAAGAAGACTTC3'; E1:C₃+1 (C74S/Y75C): 5'GGGAAAAAATGGTTCACAGGAGACGCTG3'; E1:C₁-2 (C63S/F61C): 5'GGGTGTAGAGATGCAAGAAGACTTC3'; E1:C₃+2 (C74S/N76C): 5'GGGA-AAAAATGGCAATAGGAGACGCTG3'; extracellular loop 2 (E2):C₁-1 (C178S/K177C): 5'GAAGGCCTCAGAGCAGACACCGCCG3'; E2:C₃+1 (C189S/F190C): 5'CGGGACACGCAGGAGTCCACCG3'; E2:C₁-2 (C178S/V176C): 5'GGCCTCAGACTTGACAGCCGCACC3'; E2:C₃+2 (C189S/V191C): 5'GGGCGGGAGCAGAAGGAGTCCACCG3'; E2:C₁-3 (C178S/K175C): 5'GCCTCAGACTTGACACACCGCACCATTGG3'; E2:C₁-4 (C178S/R174C): 5'CCTCAGACTTGACCAGGCACACCATGGC3'; E2:C₃+3 (C189S/S192C): 5'GTGGGGCGGCACACGAGGAGTCCAC3'; and E2:C₃+4 (C189S/R193C): 5'CTCAGTGGGGCAGGACCGAAGGAGTCC3'.

Correct mutants were selected by restriction enzyme analysis when mutagenesis altered the wild-type restriction pattern, or by DNA sequencing. From the selected plaques, the observed efficiency of mutation was >90%. Mutants in E1 were removed from the M13 vector as a BsmI/NcoI fragment, whereas those in E2 were excised as a SmaI/KpnI fragment. These fragments were subcloned as a cassette into the equivalent sites of the Cx32 wild-type (wt) coding region cloned between 5' and 3' *Xenopus* β globin untranslated regions (50- and 206-bp, respectively) in the pGEM7zf (+) vector (Promega Corp., Madison, WI). All cassettes were sequenced to ensure only the desired mutation had been created.

Combinations of cysteine shifts within E1 were prepared by HgaI (New England Biolabs Inc., Beverly, MA) digestion of the Cx32 insert that was first excised from the vector by HindIII/SacI to avoid confusion from HgaI sites in the vector. HgaI separates the cysteine 63 and 74 mutagenesis sites into fragments that could be separated on 1% agarose gels before elution and purification (Gene Clean; Bio101, La Jolla, CA) and then followed by religation with the vector. Cysteine mutants within E2 could be easily combined using a BstXI site at the 5' end of the clone, and then another separating the cysteine 178 and 189 positions. Combinations of mutants between E1 and E2 could be created by excision of the 3' end of the construct as a SmaI/KpnI fragment (containing the E2 coding region) and then religating the appropriate combinations of single or double mutants.

In Vitro Transcription

The mutant Cx32 cDNAs were linearized with HincII (Promega Corp.) and then added to a transcription reaction that included 0.5 mM each of ATP, CTP, and UTP, 0.25 mM GTP, 10 mM DTT, SP6 polymerase buffer (Promega Corp.) 150 U of RNasin (Promega Corp.), 0.3 mM 5' m⁷G Cap (Amersham Corp., Arlington Heights, IL), and 35 U of SP6 RNA polymerase (Promega Corp.). After a 15-min treatment at 37°C with RQ1 DNase, the resultant cRNA was purified using an RNaid Kit (Bio 101) and then quantitated using both an optical density (OD) 260-nm measurement, and then by comparison to a DNA sample of known concentration, run on a denaturing agarose gel stained with ethidium bromide.

Xenopus Oocyte Expression System

Oocytes were dissected from *Xenopus laevis* and then the follicular cell layer was digested away with 1 mg/ml collagenase (Sigma Chemical Co.,

St. Louis, MO). The oocytes were then coinjected with 40 nl of a mixture of 0.15 μg of antisense *Xenopus* Cx38 oligonucleotide (Barrio et al., 1991; Suchyna et al., 1993) and 0.15 μg of the appropriate cRNA using an automated microinjector (Nanoject No. 3-00-203-XV; Drummond Scientific, Broomall, PA). In rare cases of persistent exogenous connexin expression, oocytes were preinjected with 0.15 μg of antisense *Xenopus* Cx38 oligo and then allowed to incubate for 72 h before injection of 0.15 μg of the appropriate cRNA. After a 24-h incubation, the vitelline envelope was stripped manually and then the two oocytes were pushed together with vegetal poles apposed.

Conductance (g_j) between two paired oocytes was recorded using a dual voltage clamp procedure (Harris et al., 1981). Current and voltage readings from two Gene Clamp 500 voltage clamp amplifiers (Axon Instruments, Inc., Foster City, CA) were digitized for storage and analysis using Pclamp 6 software (Axon Instruments, Inc.).

In a typical experimental paradigm, 20-s voltage pulses of alternating polarity were applied to one oocyte over the range of ± 10 –110 mV (in 20-mV increments) from the clamped resting potential of both oocytes (-40 ± 10 mV). Approximately 3 min was allowed between impulses. Conductance of the mutant/wt paired oocytes was recorded as a percentage of that between wt/wt paired oocytes for that experiment. For each batch of oocytes, antisense Cx38-injected oocytes were paired and recorded to determine if all endogenous coupling was effectively eliminated by the antisense oligonucleotide. In some experiments, the mutant cRNA-injected oocytes were also paired with themselves. The E2:C₁-1/C₃+1 mutants showed 2.7% of Cx32 wt conductance ($n = 2$) and E2:C₁-2/C₃+2 showed 19.5% of Cx32 wt conductance ($n = 4$). Also, nonantisense-injected oocytes were paired with the mutant cRNA injected oocytes to check for pairing with the endogenous Cx38, indicative of a change in docking specificity.

In Vitro Translation

The various Cx32 mutants were translated using the TNT-coupled expression system (Promega Corp.) consisting of 25 μl of rabbit reticulocyte lysate, 2 μl of reaction buffer, 1 μl of SP6 RNA polymerase, 1 μl of a 1-mM amino acid mixture minus methionine, 4 μl (1,000 Ci/mmol) of [³⁵S]methionine (Dupont-NEN, Wilmington, DE), 1 μl of RNasin ribonuclease inhibitor (40 U/ μl ; Promega Corp.) 1 μg of the appropriate Cx32 DNA template, and nuclease-free water to bring the final volume to 50 μl . For these reactions, 3 μl of the water was replaced with canine pancreatic microsomes (Amersham Corp.) to test whether the translation products of these mutant cRNAs is able to insert into membranes. After 2 h at 30°C, the translation products were treated with 0.1 M Na₂CO₃, pH 11.0, for 30 min at 8°C and then centrifuged for 15 min at 13,000 g . The supernatant was discarded, and then the pellet was washed again with 0.1 M Na₂CO₃ and centrifuged as before. The pellet was then resuspended in SDS sample buffer and allowed to sit at room temperature for 15 min before loading onto a 15% SDS-polyacrylamide gel. After electrophoresis, the gel was soaked in DMSO for 20 min, and 20% 2,5-diphenyloxazole (PPO) in DMSO for 1 h and then washed with water. The dried gel was exposed to a phosphorimaging cassette (model 425E using Image Quant v4.2 software; Molecular Dynamics, Inc., Sunnyvale, CA) for 1 h before reading.

For assessment of disulfide bond formation, the translations were done in the presence of canine pancreatic microsomes as described, except that 1.5 mM of oxidized glutathione (Sigma Chemical Co.) was added to ensure oxidizing conditions. The concentration of oxidized glutathione was determined through titrations in trial experiments to allow disulfide bond formation (~ 1.5 mM) but not inhibit protein synthesis (at concentrations > 3 mM). Translations were terminated after 2 h at 30°C with 20 mM *N*-ethyl maleimide to alkylate any free sulfhydryls. The microsomes were pelleted through a high salt cushion of 250 mM sucrose in 500 mM KAcetate, 5 mM MgAcetate, and 50 mM Hepes, pH7.9, by centrifugation in a TLA rotor in a tabletop ultracentrifuge (model TL-100; Beckman Instrs., Inc., Palo Alto, CA) for 10 min at 150,000 g . The pelleted microsomes were resuspended in 90 μl of trypsin digestion buffer (50 mM NH₄HCO₃, pH 7.8). Trypsin digestion was carried out on ice for 1.5 h with 1 $\mu\text{g}/\mu\text{l}$ trypsin and then terminated by adding 2 mM soybean trypsin inhibitor (Sigma Chemical Co.). The trypsinized material with membrane-protected protein fragments was pelleted again for 20 min as above, and then resuspended in 32 μl of 1 \times SDS sample buffer without 2-mercaptoethanol. The sample was divided into two equal parts; one was reduced by adding 5% 2-mercaptoethanol, whereas the other was left under oxidizing conditions. The mixture was kept at room temperature for 30 min before analysis by SDS-PAGE. Reduced and nonreduced samples were loaded

on separate gels. The dried gel was exposed to a phosphorimager cassette for several hours and then bands were quantitated after reading on a phosphorimager (425E; Molecular Dynamics, Sunnydale, CA)

Results

Mutagenesis Strategy

Given both the conservation of cysteine positions in the extracellular loops of connexins and their inferred importance in the point mutagenesis study of Dahl et al. (1992), determination of the pattern of disulfide bonding within the extracellular loops is likely to be critical to understanding the structure of these domains. There is already direct evidence that at least one disulfide forms between the loops of a single connexin and none form between connexins (John and Revel, 1991; Rahman and Evans, 1991). However, with six cysteines present in these loops, even assuming all form disulfides, many combinations of linkages are possible (Fig. 1). These combinations can be grouped into two general categories. One group has only one disulfide linkage between the two extracellular loops (*A–E*), and the second consists of combinations with all three disulfides between the loops (*F* and *G*).

Dahl and colleagues had previously shown that the substitution of any one of these cysteines compromised channel function (1992). Movement of one cysteine of a pair is also likely to be incompatible with disulfide formation and would lead to nonfunctional channels. However, if both of the cysteines that are involved in a disulfide bond in the native structure are moved the same number of residues away from the original sites, the disulfide may be able to reform, leading to a rescue of channel function. The specific strategy used was site-directed mutagenesis to move the first and third cysteines (designated C₁ and C₃, respectively) within each extracellular loop (E1 and E2) a variable distance away from their wt positions. The second cysteine in each extracellular loop was not moved due to the possible critical nature of the flanking residues in forming a reverse turn in this region. Rescue of functional channels requires that movements would have to be made

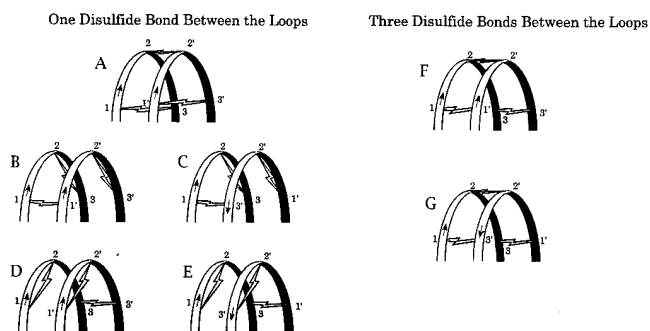


Figure 1. Possible isomers of disulfide linkages between the two extracellular loops of connexins. The conserved cysteines in the two extracellular loops of connexins are indicated, from NH₂ to COOH termini, as 1, 2, and 3 for E1 and 1', 2', and 3' for E2. The disulfide linkages, indicated by flashes, can be divided into two general categories: linkages with one disulfide between the two extracellular loops (*A–E*), and linkages with three disulfides between the two loops (*F* and *G*). Both parallel (*A*, *B*, *D*, and *F*) and antiparallel configurations (*C*, *E*, and *G*) are represented.

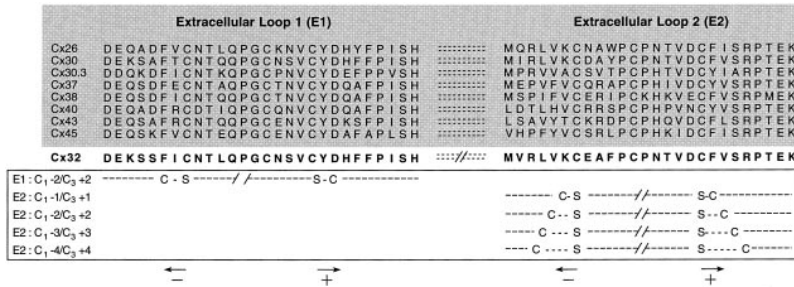


Figure 2. Schematic representation of the cysteine mutants tested. An alignment of selected mammalian connexin sequences for the two extracellular loops (E1 and E2) is shown (shaded) above the sequence of Cx32, which was the target of mutation here. Restriction enzyme sites used to create combination mutants within each loop (Fig. 3) and between loops (Fig. 4) are indicated (refer to Materials and Methods for details). Mutants leading to movement of the cysteines in E1 and E2 are illustrated, with appropriately marked arrows indicating the terminology for direction of the movements used in the text.

in compatible directions within the tertiary structure of the protein. Based on the location of C_1 and C_3 within each extracellular loop, we reasoned that this would be achieved by movements of C_1 towards the NH_2 terminus ($-$ direction) and C_3 towards the $COOH$ terminus ($+$ direction). Although in opposite directions in the primary sequence, these movements should lie in the same direction (toward the membrane) within the loops. Movements in the reverse direction (i.e., C_1 to the $COOH$ terminus and C_3 to the NH_2 terminus) were not attempted, since the spacing between C_1 and C_3 was only 10 residues. Further reduction of this spacing would be likely to interfere with the reverse turn(s) that are predicted to occur in this part of the loop.

Movements of C_1 and C_3 in both loops were made, although most extensively in E2 where sequence conservation between connexins is less stringent (Fig. 2). Restriction enzyme sites present within the Cx32 sequence allowed the creation of all possible permutations of double and some quadruple mutants. cDNA constructs were transcribed and then the cRNAs were injected into stage VI *Xenopus laevis* oocytes before pairing with like oocytes, or oocytes expressing Cx32 wt. The latter was used as the primary form of comparison, as these pairs typically gave higher conductances by not compounding potential folding defects in the mutants that might reduce efficiency of channel formation. Preinjection of antisense oligonucleotides to XeCx38 was used throughout to eliminate endogenous coupling (Barrio et al., 1991). Conductances, as measured by a dual whole cell voltage clamp, are presented as a fraction of the conductance between Cx32 wt pairings using the same oocyte batch in the same week.

Given the conserved nature of the primary sequences of the extracellular loops among connexins, it might be expected that many mutants in this series would be nonfunctional for reasons other than inappropriate disulfide formation. We attempted to minimize this by using a conservative substitution of serine for cysteine (retaining both similar side chain volume and polarity). Furthermore, substitution of cysteine for a variety of other residues in several recent cysteine-scanning mutagenesis studies have usually shown minimal perturbation of channel structure, as measured by functional properties (Akabas et al., 1994; Kurz et al., 1995).

Patterns of Coupling: Intraloop Movements

As predicted above, all of the single cysteine movements in either E1 or E2 showed little or no conductance ($<1\%$ of Cx32 wt conductance) (Fig. 3). However, analysis of the

double cysteine mutants C_1 and C_3 revealed very instructive patterns of rescue (Figs. 3 and 4). In movements within a single loop, C_1-2/C_3+2 mutants were most effective, giving values of 36 (E2) and 28% (E1) of wild-type conductance (Fig. 3). The C_1-1/C_3+1 movements in E2 yielded only 7% of wt conductance, and moves to a greater distance (C_1-3/C_3+3 and C_1-4/C_3+4) gave no and minimal coupling, respectively. Effectiveness of moves two residues away from the original location, compared to those of one or three residues away, demonstrates that rescue of function does not correlate simply with the distance of the movement in the primary sequence, but indicates a preference for a certain periodicity. This suggests the involvement of a repeating secondary structure, with the periodicity of two suggesting β sheet. The successful pairing of compatible movements within a loop initially suggested that C_1 and C_3 may be connected by an intraloop disulfide

E1		E2				%WT/SE	(n)		
C_1	C_3	C_1	C_3	10	20			30	40
		-1						0	(4)
			+1					0	(4)
		-2						0	(4)
			+2					0.9/0.3	(2)
		-3						0	(5)
			+3					0	(5)
		-1	+/-1					7.3/1.8	(6)
		-2	+/-2					36/6.6	(7)
		-3	+/-3					0	(4)
		-4	+/-4					0.6/0.3	(8)
-2								0.07/0.01	(4)
	+2							0	(4)
-2	+2							28/13.8	(8)

Figure 3. Functional analysis of single and paired movements of cysteines 1 and 3 within E1 or E2 of Cx32. Mutants of Cx32 in which cysteines 1 and 3 of either E1 or E2 were moved singly, or in pairs within a loop (refer to Fig. 2 for nomenclature used), were tested for function in paired *Xenopus* oocytes. In all cases, mutant cRNA was injected into one oocyte, and Cx32 wt cRNA into another, before pairing and analysis of coupling. The percent of mutant/Cx32 wt coupling compared to Cx32 wt/Cx32 wt coupling of oocytes from the same batch is illustrated graphically, and numerically (right), along with the standard error (SE), and number of experiments (n). Single mutants failed to pair with Cx32, as did most double movements except those in which the cysteines were moved two residues away from their original positions in the sequence.

E1		E2								%WT/SE	(n)
C ₁	C ₃	C ₁	C ₃	10	20	30	40	50	60		
-2										0.07/0.01	(4)
+2										0	(4)
	-2									0	(2)
	+2									0.9/0.3	(2)
-2		-2								0	(4)
-2			+2							47.7/15.4	(8)
	+2		+2							2.6/1.5	(3)
	+2	-2								40.1/15.1	(7)
-2	+2									28/13.8	(8)
		-4	+4							0.6/0.3	(8)
-2	-2	-4	+4							48/24.9	(5)

Figure 4. Functional analysis of paired movements of cysteines 1 and 3 between E1 and E2 of Cx32. Movements of one or both of cysteines 1 and 3 in E1 were combined in several permutations with equivalent movements of cysteines in E2 as indicated. Functional analysis in the paired oocyte expression system was as described in Fig. 3, with mutant Cx32 wt coupling expressed as a percentage of Cx32 wt/Cx32 wt coupling. The mean percent coupling/standard error and the number of experiments (*n*) are shown on the right. Interloop pairings of both C₁s or both C₃s failed to couple, but movements of C₁ in one loop and C₃ in the other consistently gave equal or better coupling than the intraloop pairings. As with the movements within a loop, a periodicity of two was evident in the functional mutants. Note that the minimally functional E2:C₁-4/C₃+4 mutant was rescued when combined with E1:C₁-2/C₃+2.

(i.e., Fig. 1 A). However, if these cysteines were involved in interloop disulfides (Fig. 1, *F* and *G*), movement of both within one loop could still be compatible with reestablishment of the disulfides if the two loops formed stacked β sheets that could slide with respect to one another over a single β sheet repeat distance. This possibility could only be definitively tested by pairing cysteine movements between the two loops.

Patterns of Coupling: Interloop Movements

All combinations of + and -2 movements of C₁ and C₃ in both the E1 and E2 loops were tested (Fig. 4). Mutants that paired movements of either both C₁s or C₃s of each loop (E1:C₁-2/E2:C₁-2 or E1:C₃+2/E2:C₃+2, respectively), combinations that might be expected to function in a parallel loop model (Fig. 1 *F*), showed no functional conductance. In contrast, mutants combining movements of C₁ and C₃ between loops (E1:C₃+2/E2:C₁-2 or E1:C₁-2/E2:C₃+2) produced robust conductances that were 40.1 and 47.7% of Cx32 wt, respectively (Fig. 4). This efficient rescue of a cysteine movement in one loop with a compensatory move in a different loop (separated by >100 amino acids in the primary sequence) cannot readily be reconciled with intraloop disulfide formation such as seen in Fig. 1 A. Rather, it is consistent with two interloop disulfides between the first and third cysteines of each loop (i.e., Fig. 1 *G* with antiparallel loops). As alluded to above, the less efficient rescue seen with paired movements within a loop could be accommodated through a sliding of the two loops with respect to one another, or a reorientation of the disulfide bonds. This would allow the disulfide to reform between residues that were originally one repeat behind one another in the wt structure. This is most easily understood

in the context of the model shown in Fig. 9 and discussed below.

A test of this deduction was suggested by our earlier data. Whereas the double mutants in E2 had shown a periodicity consistent with a β sheet conformation, movements four residues away from the original site of the cysteines had produced minimal conductance. In light of the apparent interloop nature of the disulfides, this could reflect a limited tolerance to the allowed sliding of loops with respect to one another that remains compatible with reformation of the disulfide while maintaining a tertiary structure that allows for functional docking of connexins. A prediction of this hypothesis is that compensatory movements of the cysteines in E1 could alleviate this problem. Thus, a quadruple mutant was created that combined E1: C₁-2/C₃+2 with E2:C₁-4/C₃+4. This resulted in a robust conductance of 48% of Cx32 wt, confirming that separation of the cysteines in the two loops by one β sheet repeat distance, but not two, can be accommodated (Fig. 4). It also demonstrated that the periodicity of two that was seen with the double mutants in E2 also applies to E1/E2 mutant combinations, extending at least four residues away from the original cysteine positions.

Membrane Insertion, Topology, and Disulfide Bond Formation of Mutant Connexins

As many of the mutants failed to make functional channels, we tested whether or not they were competent to make protein, insert it appropriately into membranes, and form disulfides between the extracellular loops as has been demonstrated for Cx32 wt. Constructs were added to a coupled transcription/rabbit reticulocyte lysate translation system supplemented with dog pancreatic microsomes as described elsewhere (Zhang et al., 1996). All mutants tested produced the appropriately sized translation product, along with a truncated product arising from cryptic signal peptidase cleavage (also seen with Cx32 wt; Falk et al., 1994; Zhang et al., 1996), both of which inserted into the microsomal membranes (Fig. 5). The single exception

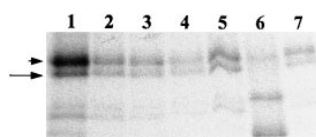


Figure 5. Cell-free translation and membrane insertion of Cx32 mutants. cRNAs for Cx32 wt, (lane 1) and a subset of the nonfunctional Cx32 cysteine mutants (lanes 2-7)

were translated in rabbit reticulocyte lysate supplemented with [³⁵S]met and dog pancreatic microsomes (Zhang et al., 1996). Microsomal pellets were isolated and then washed in Na₂CO₃ to remove accessory proteins before solubilization for SDS-PAGE and autoradiography. Cx32 wt and all mutants, except Cx32 (E1:C₁-2); (lane 6), produced two major bands corresponding to full-length Cx32 and a truncated form arising from cleavage at a cryptic signal peptidase site (Falk et al., 1994; Zhang et al., 1996), indicating insertion of all products into the membrane. Lower molecular weight products that are likely to be the result of internal initiation or premature termination of translation are evident in all translations. Cx32 (E1:C₁-2) (lane 6) produces less full-length product and a major lower molecular weight product distinct from other constructs. Samples shown are: wt Cx32 (lane 1), Cx32 (E2:C₁-1) (lane 2), Cx32 (E2:C₃+1) (lane 3), Cx32 (E2:C₁-2) (lane 4), Cx32 (E2:C₁-3/C₃+3) (lane 5), Cx32 (E1:C₁-2) (lane 6) and Cx32 (E1:C₃+2) (lane 7).

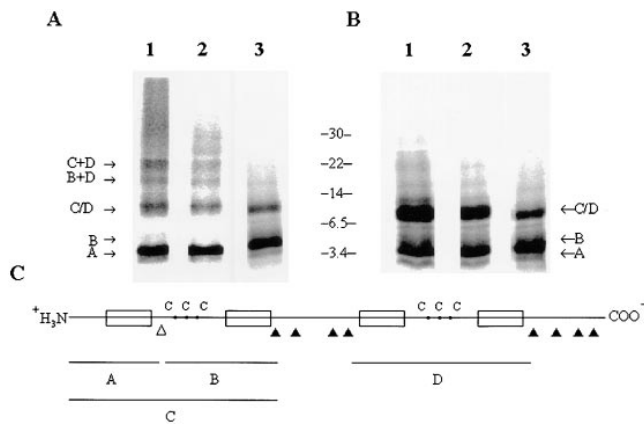


Figure 6. In vitro analysis of disulfide formation in WT and mutant Cx32. Nonreducing (A), and reducing (B) SDS-PAGE were used to dissect disulfide formation in Cx32 wt (A and B, lanes 1), functional paired mutants [Cx32 (E1:C₃+2/E2:C₁-2): A and B, lanes 2], and nonfunctional single mutants [Cx32 (E2:C₁-2) in A and B, lanes 3] produced by the cell-free translation/microsomal translocation system (Zhang et al., 1996). Full-length products were digested with trypsin albumenally (exposed sites based on wt topology are indicated by solid arrowheads in C). In combination with the cryptic activity of signal peptidase (open arrowhead), this should yield fragments A–D as indicated in C. Products were then analyzed on nonreducing (A) or reducing (B) SDS–polyacrylamide gels, with the predicted mobilities of each fragment indicated. Wt and both mutants yielded the same predicted profile under reducing conditions (B), indicating a similar topology in all cases. This pattern did not change for the nonfunctional mutant under nonreducing conditions (A, lane 3). In contrast, both wt and functional mutants yield higher molecular weight products under nonreducing conditions, consistent with disulfide formation between the loops (A, lanes 1 and 2).

was E1:C₁-2 (Fig. 5, lane 6), which showed significantly reduced insertion of the full-length product into membranes, and a concomitant lack of cryptic signal cleavage. Accumulation of low molecular weight products suggested that this mutant was more prone to proteolysis, perhaps as a result of inappropriate folding. In general, however, the results demonstrate that most nonfunctional mutants retain their ability insert into membranes as full-length products, although with variable efficiency (Fig. 5, lanes 2 and 4).

This cell-free system could also be used to examine the topology of the mutant proteins in the membrane (Zhang et al., 1996), and directly test their ability to form disulfide bonds between the extracellular loops once the appropriate oxidizing conditions are established in the microsomes (Yilla et al., 1992; refer to Materials and Methods). Trypsin digestion of Cx32 in isolated gap junction plaques (Nicholson et al., 1981; Zimmer et al., 1987) or after insertion into microsomes in the cell-free system (Zhang et al., 1996), yields two membrane-protected fragments of ~11 kD under reducing conditions (Fig. 6 B, bands C/D). Although SDS-PAGE does not resolve these, sequencing (Nicholson et al., 1981; Hertzberg et al., 1988) and immunolabeling (Milks et al., 1988; Zhang et al., 1994) has individually identified them. In addition, poorly resolved fragments of 5- and 6-kD are also seen in tryptic digests of Cx32 wt in the cell-free system (Fig. 6 B, bands A and B). The relative

Table I. Comparison of Disulfide Bond Formation in Microsomes for Cx32 wt and Functional and Nonfunctional Mutants

Construct	Mean ratio*	Number of experiments	SE	P value cf. Cx32 wt
Cx32, wt	2.66	5	0.32	—
Cx32/E1:C ₃ +2, E2:C ₁ -2	3.12	4	0.40	<0.05
Cx32/E1:C ₁ -2, E2:C ₃ +2	3.29	3	0.45	<0.05
Cx32/E2:C ₁ -1	0.94	3	0.26	>0.05
Cx32/E1:C ₁ -2	1.30	2	0.05	>0.05
Cx32/E1:C ₃ +1	1.54	2	0.05	>0.05

*Ratio of the percentage of oxidized forms of trypsinized connexins seen in nonreducing and reducing gels.

‡P value, determined by Student's *t* test, to assess the probability that the result obtained is the same as seen in Cx32 wt channels.

intensity of the A and B bands compared to the C/D band has been found to correlate closely with the degree of aberrant signal peptidase cleavage associated with different microsomes preparations (data not shown), suggesting that fragments A and B are derived from fragment C. (Fig. 6 C). All of the mutant connexins described here, including those that fail to produce functional channels, display this same pattern (Fig. 6 B; compare lanes 2 and 3 with 1). This strongly argues that these mutant proteins not only insert into membranes, but do so with the appropriate topology.

In isolated gap junction plaques, John and Revel (1991) and Rahman and Evans (1991) had first demonstrated that disulfide(s) link the COOH- and NH₂-terminal tryptic fragments of Cx32 to yield a higher molecular weight species in nonreducing SDS-PAGE. When trypsinized microsomes from cell-free translation of Cx32 were run on similar nonreducing gels, this same pattern is consistently seen with either Cx32 wt or the cysteine mutants that form functional channels (Fig. 6 A, lanes 1 and 2, respectively). In marked contrast, no higher molecular weight forms were detected in the Cx32 cysteine mutants that fail to form functional channels (Fig. 6 A, lane 3). The actual banding pattern was complicated by the aberrant cleavage that occurs in the microsomes, since not only do fragments C and D cross-link (Fig. 6; producing a 22-kD band), but also fragments B and D (Fig. 6; producing a 17-kD band). The formation of the higher molecular weight species in going from reducing (Fig. 6 B) to oxidizing (Fig. 6 A) conditions occurred concomitant with a depletion of bands B and C/D (Fig. 6), whereas band A, predicted to contain no cysteines (Fig. 6 C), was unaffected.

These results were quantitated using phosphoimager software and then the percent of total connexin protein represented by oxidized material was calculated (density of 22- and 17-kD bands/density of 22-, 17-, 11-, 6-, and 5-kD bands). The ratios of these percentages in nonreducing and reducing gel profiles of the same experiment are shown in Table I. These values demonstrate a strict correlation between the paired cysteine movements that restore functional channels and those that are compatible with disulfide formation between the extracellular loops, as seen in Cx32 wt. The fact that individual movements of either C₁ or C₃ in either loop causes disruption of the disulfides connecting the loops lends direct biochemical support for Fig. 1, F or G.

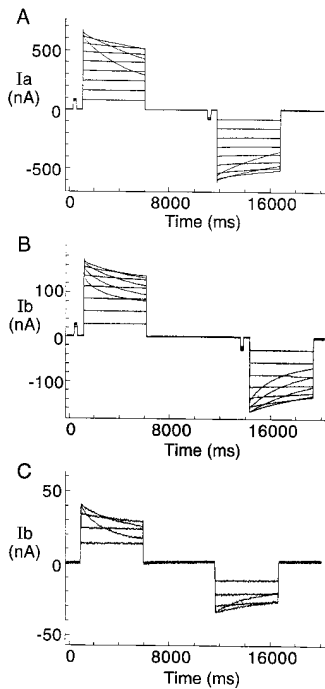


Figure 7. Current traces of wt and mutant Cx32 channels express in *Xenopus* oocyte pairs. As a test of the degree to which mutant Cx32 channels reproduced the wt channel phenotype, transjunctional currents in response to applied transjunctional voltage steps from -100 to $+100$ mV in 10 -mV (*A* and *B*) or 20 -mV (*C*) increments were recorded in the paired *Xenopus* oocyte system. Oocytes were initially clamped at -40 mV. 3 min was allowed for recovery between pulses. Responses of the wt channels (*A*) were essentially indistinguishable in kinetics and sensitivity to voltage from either heterotypic pairings of Cx32 wt and Cx32 (E1:C₃+2/E2:C₁-2) (*B*) or homotypic pairing of Cx32 (E1:C₃+2/E2:C₁-2). However, progressive decreases in the absolute conductance level of the mutant were typically observed. Similar results were obtained with other functional mutants listed in Figs. 3 and 4.

absolute conductance level of the mutant were typically observed. Similar results were obtained with other functional mutants listed in Figs. 3 and 4.

Mutant Channel Properties and Specificity

In addition to investigating the possible causes contributing to the failure of mutants to form functional channels, it is also essential to determine whether the functional mutants reestablish channel structures that are similar to the native one. Previous studies have shown the voltage-gating response of Cx32 channels to be highly sensitive to minor perturbations of the structure (Rubin et al., 1993; Suchyna et al., 1993; Verselis et al., 1994). Thus, this parameter should serve as a sensitive indicator of the native configuration of the protein. Functional cysteine mutants showed voltage-gating characteristics indistinguishable from wild-type (Fig. 7 *A*) in terms of both the sensitivity and kinetics of their responses to incremental hyper- and depolarizing voltage pulses. This was true whether homotypic (Fig. 7 *B*) or heterotypic combinations (Fig. 7 *C*) were compared. Therefore, even though we have moved the position of the cysteines and the position of the disulfide bond, we have not significantly modified channel properties, or, by inference, the overall channel structure.

In the course of these studies we encountered one surprising finding involving the mutant E2:C₁-2 alone, or in combination with E1:C₁-2. Based on the previous results, these two cysteines (the first in each extracellular loop) would not be expected to form a disulfide bond, and thus neither mutant should be functional. Consistent with this prediction, neither mutant formed functional channels with Cx32 wt. However, on pairing with oocytes that had not received antisense oligonucleotides against XeCx38, it was found that both mutants readily formed channels with the endogenous oocyte connexin (Fig. 8; XeCx38). Func-

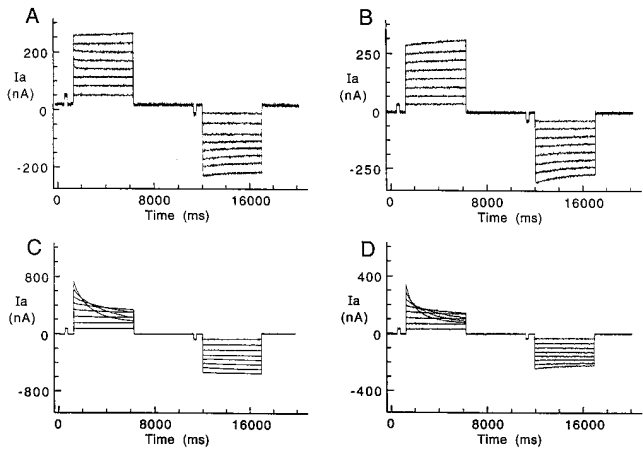


Figure 8. Current traces of Cx32 mutants E2-2 and E1-2/E2-2 paired with an oocyte expressing the endogenous connexin (XeCx38). Shown are plots of current (nA) versus time (ms) for oocyte pairs injected with Cx32 (E2:C₁-2): water (*A* and *C*), and Cx32 (E1:C₁-2/E2:C₁-2): water (*B* and *D*). Currents are in response to 20 -s transjunctional voltage steps from -110 to $+110$ mV in 20 -mV increments. The majority of records obtained show little or no response of junctional currents to transjunctional voltage gradients in this range (*A* and *B*). In one experiment, a markedly asymmetric response was noted for both mutants (*C* and *D*). One side remained voltage insensitive, but when the XeCx38-expressing cell was relatively positive, a fast and sensitive voltage response was seen analogous to that of XeCx38 homotypic channels.

tional coupling with XeCx38 was never detected with Cx32 wt (Barrio et al., 1991), although it is a property associated with some other mammalian connexins (e.g., Cx43). In the case of Cx32 (E2:C₁-2), 76% of the pairings with uninjected oocytes developed conductance to levels $52 \pm 10\%$ of that between Cx32 wt pairs. Similarly, 45% of the pairings between Cx32 (E1:C₁-2/E2:C₁-2) and uninjected oocytes showed coupling that averaged $46 \pm 17\%$ of the mean conductance between Cx32 wt pairs. The coupling seen with both mutants was demonstrated to be attributable to induction of XeCx38, as it could be eliminated by preinjection of an antisense oligonucleotide to XeCx38 (Figs. 3 and 4). Possible complications that could arise from cooligomerization of the Cx32 mutants and XeCx38 within the same oocyte were eliminated by the presence of antisense oligonucleotides in all mutant and wt Cx32-expressing cells.

The failure of a significant fraction of tested pairs to couple in the cases of these latter mutants is likely to be attributable, in part, to variability in the endogenous stores of XeCx38. Even in the well-documented case of Cx43 wt pairing with XeCx38, only 85% of cell pairs couple. Differences in the coupling frequencies seen between mutants could have several explanations, although a likely possibility is that it reflects differences in the efficiency of folding or assembly of the mutant proteins at the lower temperatures used with *Xenopus* oocytes.

As noted above, all connexin mutants tested here that could pair with Cx32 wt showed symmetrical current profiles over a range of voltages that were very analogous to responses of Cx32 wt injected pairs (Fig. 7). In marked

contrast, the E2:C₁-2 and E1:C₁-2/E2:C₂-2 mutant pairings with XcCx38 showed a surprising absence of voltage sensitivity to ± 110 mV (Fig. 8, *A* and *B*), even on the side in which XcCx38 was expressed. This clearly carries implications for a strong influence of the docking process on voltage gating that are discussed further below. In one out of seven batches of oocytes tested (4 out of 56 pairs), we did see asymmetric voltage sensitivity with relatively rapid drops in conductance when the XcCx38 oocyte was relatively positive, but no voltage-induced decrements in currents when the Cx32 mutant-expressing cell was relatively positive (Fig. 8, *C* and *D*). This was seen with both mutants ($n = 2$ for each). No overt explanation for the disparate behavior of this batch of oocytes was evident. However, given the potential for these mutants to misfold, it is possible that the complex proofreading that occurs during membrane protein biosynthesis may show differences between oocyte batches.

Discussion

We have used a novel approach to defining structural features of a membrane protein that is not well suited to analysis by traditional approaches. The extracellular loop regions of connexins are similar in function, but not structure, to the homophilic binding domains of cadherins and the IgG class of cell adhesion molecules. Thus, gap junctions represent a third class of cell-cell recognition proteins that are likely to use unique paradigms for homo- and heterophilic interactions. Furthermore, understanding the structure of the extracellular loop regions of gap junction proteins is a key step to unraveling the process of hemichannel docking that is required for the formation of the extracellular extension of the gap junction channel. This is a unique process, not only in terms of the electrically tight seal that is formed, but also because of its specificity. This allows selective formation of heterotypic gap junctions between different members of the connexin family (Elfgang et al., 1995; White et al., 1995).

The experiments presented here have taken the first step to elucidating this structure by defining the disulfide bonding pattern within these extracellular loops. The conserved and critical nature of these cysteines suggests that they play an important role in defining and stabilizing the structure of these regions. Previous studies had already established that deletion of the cysteines individually destroys channel function (Dahl et al., 1992). Hence, the strategy we chose involved moving the position of the cysteines singly, in pairs, or even quadruplets within the extracellular loops. The expectation was that paired movements of the appropriate cysteines could rescue defects caused by single mutants by allowing disulfide bonds to be reestablished without overt disruption of the loop structure. The validity of this strategy was directly documented in a cell-free translation/translocation system that showed a close correlation between functional mutants and formation of interloop disulfides (refer to Fig. 6 and Table I).

Disulfide Connections Suggest a Model of Connexin Extracellular Domains

All of the data presented here suggest a model in which

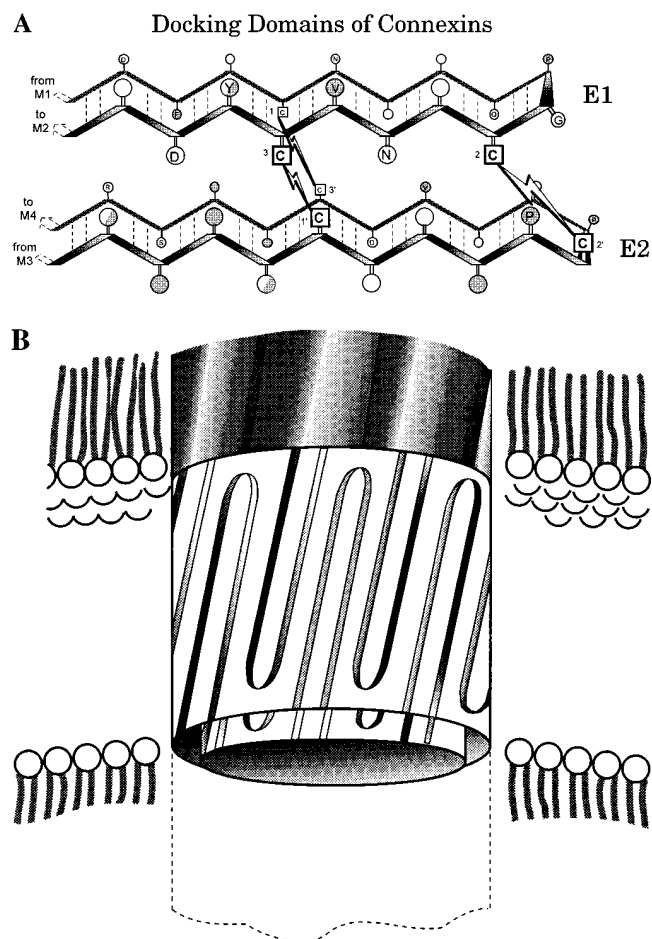


Figure 9. Proposed model of the extracellular loop regions of a connexin. (*A*) Based on the observations presented here, E1 and E2 form stacked, antiparallel β sheets connected by three disulfide bonds, although the bond between the 2 and 2' cysteines is not directly demonstrated here. The model accounts for the periodicity of cysteine movements between loops that rescue coupling, and how movements of the first and third cysteines within a loop could be accommodated by a change in the orientation of the interloop disulfides, or a sliding of the loops with respect to one another. Equivalent loops from the connexins of the apposed hemichannel are hypothesized to interdigitate in front of and behind the stacked loops shown. Conserved residues are indicated based on alignments of all vertebrate connexins. Filled circles indicate hydrophobic character, and open circles indicate hydrophilic character. Half-filled circles indicate that either no consensus of hydrophilic or hydrophobic residues exists at this location, or the conserved residue at that location has an amphipathic character (e.g., Y). Specific residues are only indicated when at least 14 of the 17 aligned sequences were identical at that position. (*B*) An artist's impression of the β zip model of how the loops of individual connexins could interdigitate to form a β barrel extension of the gap junction channel at the docking interface between hemichannels. Concentric barrels, according to the model shown in *A*, would be held together by disulfides and are shown extending from the connexin subunits within the membrane into the extracellular space separating the cells. The loops have been shown with an arbitrary tilt to the perpendicular axis of the barrel, consistent with other known β barrel structures.

the two extracellular loop regions form stacked antiparallel β sheets (Fig. 9). The reverse turn is placed in the conserved, proline-glycine-rich region near the second cysteine in each loop. The loops are joined and held in a fixed conformation with two, or possibly three, interloop disulfides. Two disulfides appear to form between the first and third cysteines from each loop (C_1 and C_3). Whether the remaining two cysteines (the C_2 s) also form an interloop disulfide is not directly tested here.

In the model shown in Fig. 9, the proposed β sheet structure is based on the periodicity of two seen in the paired cysteine movements that are compatible with gap junction function. These movements are inconsistent with an α helical structure of these loops, and do not readily reconcile with a random coil conformation. The highly efficient rescue achieved by mutants (E1: C_3+2 /E2: C_1-2) and (E1: C_1-2 /E2: C_3+2) in which the first cysteine of one loop and the third of the other are moved in concert, but in opposite directions in the primary sequence, can only readily be reconciled with disulfide linkages between the loops that are arranged in an antiparallel manner. The only other possibility to explain this result would be a rearrangement of the disulfide linkages within both loops. This seems inconsistent with the nonfunctional nature of the single mutants that would undergo identical rearrangements within a single loop. The partial rescue affected by paired mutants within a loop would not require rearrangements within each loop. It could be accounted for by reorientation of the disulfide bond (i.e., pairing with the residue one repeat behind instead of one repeat ahead in the adjacent β sheet, see Fig. 9) and/or a sliding of the loops with respect to one another by a single β sheet repeat distance. Both of these are likely to represent minimal perturbations to the overall structure. This explanation is supported by the failure of the E2: C_1-4 / C_3+4 mutant to support coupling, but its robust coupling when combined with a compensatory movement of cysteines within E1 (i.e., E1: C_1-2 / C_3+2). This result underscores the limited tolerance of this structure to modification, as sliding of the loops with respect to one another cannot occur over more than one repeat distance of the β sheets and remain consistent with assembly of functional channels.

In deriving this model, native disulfide bond formation was deduced from functional assembly of gap junctions as measured by the electrical coupling of oocytes. However, in several cases this was also directly tested biochemically in a cell-free translation system. An exact correlation was found between interloop disulfide bond formation, as seen in Cx32 wt, and paired cysteine movements that resulted in functional coupling of oocytes. Surprisingly, no interloop disulfides could be detected in any of the nonfunctional mutants that were tested. Several of these were single mutants (see Table I) in which five of the six cysteines were undisturbed. Thus, one might have predicted one or two interloop disulfides to remain. However, it is also possible that the odd number of cysteines available for pairing could lead to competition, producing inappropriate disulfides that may be intraloop, or unstable, and hence undetectable in the assay system we used. This underscores the importance of a conservation of all six cysteines in the connexin family, and the critical role of the disulfides in stabilizing loop structure.

The overall arrangement of the extracellular loops reported here also carries clues as to the packing of the four transmembrane regions within the cell membrane. It has been previously proposed, but never documented, that the four transmembrane segments are arranged sequentially in a clockwise manner (Milks et al., 1988). This is based on analogies with other α helical bundle proteins such as keratin or bacteriorhodopsin, but has not been directly demonstrated. The antiparallel configuration of the loops inferred from the current data, however, dictates that the transmembrane segments must be arranged in sequential order from the NH_2 to $COOH$ terminus. Although no distinction can be made between clockwise or counterclockwise configurations, amino acid chirality would suggest the former as the likely model. Overall, this leads to a significant simplification of the model building process of gap junctional structure (Peracchia et al., 1994).

Mutants Retain Most WT Properties

The functional mutants tested here showed no significant differences from Cx32 wt in their voltage-gating properties (Fig. 7). The parameters of gap junctional responses to transjunction voltage differences have already proven highly sensitive to mutation in several parts of the molecule, including E1 (Rubin et al., 1992; Verselis et al., 1994). Thus, the retention of wt gating responses to transjunctional voltage differences would suggest mutants that still pair with Cx32 retain most of their original structural features.

However, even in the best cases, mutants rarely displayed >50% of the wt coupling. This may have several causes, not the least of which could be the replacement of highly conserved residues within the extracellular loops with cysteine in several of the mutants tested (refer to alignments shown in Fig. 2). In addition, it is possible that folding of the mutant polypeptides and their transport to the cell surface could have a reduced efficiency in the oocyte that was not evident in the cell-free system. One would predict that such reduced efficiency would be compounded in cases where the mutant is expressed in both cells of a pair, as compared to mutant/wt pairings. Consistent with this prediction, mutant connexins paired with themselves produced only half of the coupling seen in pairings of the mutant with Cx32 wt (i.e., 19.5 and 36%, respectively, in the case of E2: C_1-2 / C_3+2 ; also see Fig. 7 for a similar comparison of the E1: C_3+2 /E2: C_1-2 mutant).

Specificity of Connexin Docking Is Influenced by Tertiary Structure

The importance of the appropriate folding of the extracellular loops to the specific docking between connexins was graphically illustrated by two cysteine mutants that would be expected to be nonfunctional based on the model shown in Fig. 9. Although the single mutant E2: C_1-2 and the double mutant E1: C_1-2 /E2: C_1-2 (that paired movements of C_1 in both loops) both failed to form functional channels with Cx32 wt as predicted, they were able to pair efficiently with endogenous XcCx38. This is not a property of Cx32 wt, yet neither of these mutants involve significant changes in the primary sequence of the extracellular loops that determine docking specificity (White et al., 1994,

1995). However, the unmatched movements of the cysteines might be expected to cause significant distortion of the normal folding motifs of these loops. In fact, E2:C₁-2 did not form detectable interloop disulfides in our cell-free translation system (Fig. 6). Thus, this result strongly suggests that docking specificity is not merely a function of primary sequence, but is influenced significantly by the tertiary structure of the loop domains, influenced in this case by disulfide formation.

Such a conclusion is consistent with the results of chimera between Cx40 and -43 reported by Haubrich et al. (1996) and comparisons of these same chimera in the oocyte system (Zhu, H., and B.J. Nicholson, unpublished observations). In both cases, the heterotypic pairing properties were not dictated only by the origin of the extracellular loops, but also by the origin of the transmembrane and cytoplasmic domains to which they were attached. Our findings may also explain why Cx31, which has a different spacing of cysteines to all other connexins, fails to form functional channels with other connexins, but can dock with itself (Elfgang et al., 1995).

Docking Significantly Influences the Transjunctional Voltage Gate

The E2:C₁-2 and E1:C₁-2/E2:C₁-2 mutants also graphically demonstrate the influence of the structure of the extracellular domains on the voltage gating characteristics of gap junctions. The novel interaction between both of these mutants and XeCx38 resulted in complete suppression of the voltage sensitivity of both Cx32 and XeCx38 (Fig. 8, A and B). Modification of the gating characteristics of several connexins when they are combined heterotypically has been reported previously (Hennemann et al., 1992; White et al., 1994), although not to the extent of the complete suppression that is seen here. Several mutations of residues in E1 have also been associated with changes in the voltage gating profile of Cx32 and Cx26, an effect that could be mediated by modifications of channel docking (Rubin et al., 1992). In fact, the docking process itself must form a part of the transjunctional voltage sensor. More direct evidence of this is provided by a comparison of the voltage responses of Cx46 in the hemichannel and the intact gap junctional form. Both show responses over similar voltage ranges, but the polarity of the response is reversed upon docking of the hemichannels (Ebihara et al., 1990).

Models of Docking and the Structure of Channels Spanning Gaps

From our model (Fig. 9), it is now possible to propose a self-consistent hypothesis of how such a configuration of the extracellular loops might dock with an apposed connexin. We propose a model in which the extracellular loops of each connexin in a hemichannel would interdigitate with the extracellular loops from the hemichannel in the adjacent cell, rather like the two sides of a zipper. This interdigitation of the extracellular domains is also supported by structural studies of both hemichannels (Perkins et al., 1997) and intact gap junctional plaques (Unger et al., 1997). Although the docking structures have not been directly imaged, both studies conclude that a model involving stag-

gering of the subunits of apposed connexins leading to an interdigitation of the extracellular domains is most easily reconciled with the data.

The interleaved β sheets in our model would form an antiparallel β barrel motif we term a " β zip", which could provide a sealed extracellular extension of the channel required for passage of ions and small molecules between cells. This model is somewhat akin to bacterial porin (Jap et al., 1991; Weiss et al., 1991), but in this case the barrel would have 24 strands and two concentric layers (one formed by E1 loops, the other by E2 loops), with different subunits providing the β strands. In the current model, the two concentric barrels have the same number of strands. This would seem inconsistent with their different diameters. One possible solution to this apparent anomaly would be for the outer barrel not to form a continuously hydrogen bonded structure, but have a greater spacing between strands contributed by different connexins. The surrounding water could then take up the lost H bonds.

The 30-amino acid extracellular loops could maximally form two 13-residue β strands connected by a minimal reverse turn. This would extend ~ 30 Å into the gap, necessitating a significant degree of interdigitation of β sheets from apposed connexins, although the degree of such overlap would be influenced by any tilt of the β sheets from the perpendicular to the membrane. The extensive H bonding that would occur between β strands contributed by apposed connexins is consistent with the requirement for high urea concentrations in the splitting of gap junction membranes (Manjunath et al., 1984). Other configurations of β sheet structures would be consistent with the data presented here and the dimensions of the extracellular domains of connexins. However, none of these form structures that have been associated with channel-like structures (Jap et al., 1991; Weiss et al., 1991). Definitive conclusions as to the structure of these docking domains must await direct structural analysis, but the current hypothesis poses a testable model on which to predicate future analyses of docking specificity and the nature of the unique ion-tight seal formed at the docking interface between connexins.

We would like to thank J. Stamos (SUNY, Buffalo, NY) for the preparation of the artwork and figures.

This work was supported by National Institutes of Health grants (grant numbers CA-48049 and HL-48773).

Received for publication 25 June 1997 and in revised form 8 January 1998.

References

- Akabas, M.H., C. Mann, P. Archdeacon, and A. Karlin. 1994. Identification of acetylcholine receptor channel-lining residues in the M-Z segment of the α subunit. *Neuron*. 13:919-927.
- Barrio, L.C., T. Suchyna, T. Bargiello, L.X. Xu, R.S. Roginski, M.V.L. Bennett, and B.J. Nicholson. 1991. Gap junctions formed by connexins 26 and 32 alone and in combination are differentially affected by voltage. *Proc. Natl. Acad. Sci. USA*. 88:8410-8414.
- Cascio, M., E. Gogol, and B.A. Wallace. 1990. The secondary structure of gap junctions. Influence of isolation methods and proteolysis. *J. Biol. Chem.* 265: 2358-2364.
- Caspar, D.L., D.A. Goodenough, L. Makowski, and W.C. Phillips. 1977. Gap junction structures. Correlated electron microscopy and X-ray diffraction. *J. Cell Biol.* 74:605-628.
- Dahl, G., R. Werner, E. Levine, and C. Rabadan-Diehl. 1992. Mutational analysis of gap junction formation. *Biophysics J.* 62:172-182.
- Dermietzel, R., and D.C. Spray. 1993. Gap junctions in the brain: where, what type, how many and why. *Trends Neurosci.* 16:186-192.
- Ebihara, L., V.M. Berthoud, and E.C. Beyer. 1995. Distinct behavior of Cx56 and Cx46 gap junctional channels can be predicted from the behavior of

- their hemi-gap junctional channels. *Biophys J.* 68:1796–1803.
- Elfgang, C., R. Eckert, H. Lichtenberg-Frate, A. Butterweck, O. Traub, R.A. Klein, D.F. Hulser, and K. Willecke. 1995. Specific permeability and selective formation of gap junction channels in connexin-transfected HeLa cells. *J. Cell Biol.* 129:805–817.
- Falk, M.M., N.M. Kumar, and N.B. Gilula. 1994. Membrane insertion of gap junction connexins: polytopic channel-forming membrane proteins. *J. Cell Biol.* 127:343–355.
- Fulton, B.P. 1995. Gap junctions in the developing nervous system. *Dev. Neurobiol.* 2:327–334.
- Ghoshroy, S., D.A. Goodenough, and G.E. Sosinsky. 1995. Preparation, characterization and structure of half gap junctional layers split with urea and EGTA. *J. Membr. Biol.* 146:15–28.
- Guthrie, S.C., and N.B. Gilula. 1989. Gap junctional communication and development. *Trends Neurosci.* 12:12–16.
- Harris, A.L., D.C. Spray, and M.V. Bennett. 1981. Kinetic properties of a voltage-dependent junctional conductance. *J. Gen. Physiol.* 77:95–117.
- Haubrich, S., H.-J. Schwartz, F. Bukauskas, H. Lichtenberg-Fraté, O. Traub, R. Weingart, and K. Willecke. 1996. Incompatibility of connexin 40 and 43 hemichannels in gap junctions between mammalian cells is determined by intracellular domains. *Mol. Biol. Cell.* 7:1995–2006.
- Hennemann, H., T. Suchyna, S. Jungbluth, E. Dahl, B.J. Nicholson, and K. Willecke. 1992. Cloning and functional expression of a second connexin, Cx40, expressed highly in lung. *J. Cell. Biol.* 117:1299–1310.
- Hertzberg, E.L., R.M. Disher, A.A. Tiller, Y. Zhou, and R.G. Cook. 1988. Topology of the Mr 27,000 liver gap junction protein. Cytoplasmic localization of amino- α carboxy-termini and a hydrophilic domain which is protease hypersensitive. *J. Biol. Chem.* 263:19105–19111.
- Hoh, J.H., S.A. John, and J.P. Revel. 1991. Molecular cloning and characterization of a new member of the gap junction family, connexin-31. *J. Biol. Chem.* 266:6524–6531.
- Hoh, J.H., G.E. Sosinsky, J.P. Revel, and P.K. Hansma. 1993. Structure of the extracellular surface of the gap junction by atomic force microscopy. *Biophys. J.* 65:149–163.
- Jap, B.K., P.J. Walian, and K. Gehring. 1991. Structural architecture of an outer membrane channel as determined by electron crystallography. *Nature.* 350:167–170.
- John, S.A., and J.P. Revel. 1991. Connexin integrity is maintained by non-covalent bonds: intramolecular disulfide bonds link the extracellular domains in connexin-43. *Biochem. Biophys. Res. Comm.* 178:1312–1318.
- Kunkel, T.A., J.D. Roberts, and R.A. Zakour. 1987. Rapid and effective site specific mutagenesis without phenotypic selection. *Methods Enzymol.* 154:369–382.
- Kurz, L.L., R.D. Zuhlke, H.J. Zhang, and R.H. Joho. 1995. Side chain accessibilities in the pore of K⁺ channels probed by sulfhydryl-specific reagents after cyteine scanning mutagenesis. *Biophys. J.* 68:900–905.
- Levine, E., R. Werner, I. Neuhaus, and G. Dahl. 1993. Asymmetry of gap junction formation along the animal-vegetal axis of *Xenopus* oocytes. *Dev. Biol.* 156:490–499.
- Loewenstein, W.R., and B. Rose. 1992. The cell-cell channel in the control of growth. *Sem. Cell Biol.* 3:59–79.
- Makowski, L., D.L. Caspar, W.C. Phillips and D.A. Goodenough. 1977. Gap junction structures. II. Analysis of the X-ray diffraction data. *J. Cell Biol.* 74:629–645.
- Manjunath, C.K., G.E. Goings, and E. Page. 1984. Detergent sensitivity and splitting of isolated liver gap junctions. *J. Membr. Biol.* 78:147–155.
- Milks, L.C., N.M. Kumar, R. Houghten, N. Unwin, and N.B. Gilula. 1988. Topology of the 32-kd liver gap junction protein determined by site-directed antibody localization. *EMBO (Eur. Mol. Biol. Organ.) J.* 7:2967–2975.
- Musil, L.S., and D.A. Goodenough. 1993. Multisubunit assembly of an integral plasma membrane channel protein, gap junction connexin 43, occurs after exit from the ER. *Cell.* 74:1065–1077.
- Nicholson, B.J., M.W. Hunkapiller, L.B. Grim, L.E. Hood, and J.P. Revel. 1981. The rat liver gap junction protein properties and partial sequence. *Proc. Natl. Acad. Sci. USA.* 78:7594–7598.
- Paul, D.L. 1986. Molecular cloning of cDNA for rat liver gap junction protein. *J. Cell Biol.* 103:123–134.
- Paul, D.L., K. Yu, R. Bruzzone, R.L. Gimlich, and D.A. Goodenough. 1995. Expression of a dominant negative inhibitor of intercellular communication in the early *Xenopus* embryo causes delamination and extrusion of cells. *Development (Camb.)*. 121:371–381.
- Peracchia, C., A. Lazrle, and L. Peracchia. 1994. Molecular Models of Channel Interaction and Gating in Gap Junctions. C. Peracchia, editor. Handbook of Membrane Channels. Academic Press, NY. 361–377.
- Perkins, G., D.A. Goodenough, and G. Sosinsky. 1997. Three-dimensional structure of the gap junction connexon. *Biophysical J.* 72:533–544.
- Rahman, S., and W.H. Evans. 1991. Topography of connexin 32 in rat liver gap junctions: evidence for an intramolecular disulfide linkage connecting the two extracellular peptide loops. *J. Cell Sci.* 100:567–578.
- Rubin, J.B., V.K. Verselis, M.V.L. Bennett, and T.A. Bargiello. 1992. A domain substitution and its use to analyze voltage dependence of homotypic gap junctions formed by connexins 26 and 37. *Proc. Natl. Acad. Sci. USA.* 89:3820–3824.
- Severs, N.J. 1994. Pathophysiology of gap junctions in heart disease. *J. Cardiovasc. Electrophys.* 5:462–475.
- Sosinsky, G.E. 1992. Image analysis of gap junction structures. *Electron Microsc. Rev.* 5:59–76.
- Suchyna, T.M., L.X. Xu, F. Gao, C.R. Fourtner, and B.J. Nicholson. 1993. Identification of a proline residue as a transduction element involved in voltage gating of gap junctions. *Nature.* 365:847–849.
- Tibbitts, T.T., D.L. Caspar, W.C. Phillips and D.A. Goodenough. 1990. Diffraction diagnosis of protein folding in gap junction connexins. *Biophys. J.* 57:1025–1036.
- Unger, V.M., N.M. Kumar, N.B. Gilula, and M. Yeager. 1997. Projection structure of a gap junction membrane channel at 7 \AA resolution. *Nat. Struct. Biol.* 4:39–43.
- Unwin, P.N.T., and G. Zampighi. 1980. Structure of the junction between communicating cells. *Nature.* 283:545–549.
- Verselis, V.K., C.S. Ginter, and T.A. Bargiello. 1994. Opposite voltage gating polarities of two closely related connexins. *Nature.* 368:348–351.
- Weiss, M.S., U. Abele, J. Weckesser, W. Welte, E. Schiltz, and G.E. Schulz. 1991. Molecular architecture and electrostatic properties of a bacterial porin. *Science.* 13:1627–1630.
- White, T.W., R. Bruzzone, S. Wolfma, D.L. Paul, and D.A. Goodenough. 1994. Selective interactions among the multiple connexin proteins expressed in the vertebrate lens: the second extracellular domain is a determinant of compatibility between connexins. *J. Cell Biol.* 125:879–892.
- White, T.W., D.L. Paul, D.A. Goodenough, and R. Bruzzone. 1995. Functional analysis of selective interactions among rodent connexins. *Mol. Biol. Cell.* 6:459–470.
- Yamasaki, H., and Naus, C.C.G. 1991. Role of connexin genes in growth control. *Carcinogenesis.* 17:1199–1213.
- Yancey, S.B., S.A. John, R. Lal, B.J. Austin, and J.P. Revel. 1989. The 43-kD polypeptide of heart gap junctions: immunolocalization, topology, and functional domains. *J. Cell Biol.* 108:2241–2254.
- Yeager, M., and Nicholson, B.J. 1996. Structure of gap junction intercellular channels. *Curr. Opin. Struct. Biol.* 6:183–192.
- Yilla, M., D. Doyle, and J.T. Sawyer. 1992. Early disulfide formation prevents heterotypic aggregation of membrane proteins in a cell-free translation system. *J. Cell Biol.* 188:245–252.
- Zhang, J.T., and B.J. Nicholson. 1994. The topological structure of connexin 26 and its distribution compared to connexin 32 in hepatic gap junctions. *J. Membr. Biol.* 139:15–29.
- Zhang, J.T., M. Chen, C.I. Foote, and B.J. Nicholson. 1996. Membrane integration of in-vitro translated gap junctional proteins: co- and post-translational mechanisms. *Mol. Biol. Cell.* 7:471–482.
- Zimmer, D.B., C.R. Green, W.H. Evans, and N.B. Gilula. 1987. Topological analysis of the major protein in isolated rat liver gap junctions and gap junction-derived single membrane structures. *J. Biol. Chem.* 262:7751–7763.

